

# Kinematics of Persistent Random Walkers with Distinct Modes of Motion

M. Reza Shaebani\* and Zeinab Sadjadi

*Department of Theoretical Physics & Center for Biophysics,  
Saarland University, D-66123 Saarbrücken, Germany*

We study the stochastic motion of active particles that undergo spontaneous transitions between distinct modes of motion. Each mode is characterized by a speed distribution and an arbitrary (anti-)persistence. We develop an analytical framework to provide a quantitative link between the particle dynamics properties and macroscopically observable transport quantities of interest. For exponentially distributed residence times in each state, we derive analytical expressions for the initial anomalous exponent, the characteristic crossover time to the asymptotic diffusive dynamics, and the long-term diffusion constant. We also obtain exact expressions for the time evolution of the arbitrary moments of displacement—particularly the mean square displacement—over all time scales. Our approach enables us to disentangle the combined effects of speed, directional persistence, and switching probabilities between the states on the kinematics of particles in a wide range of multistate stochastic active/passive processes and to optimize the transport quantities of interest with respect to any of the particle dynamics properties.

PACS numbers: 05.40.Fb, 02.50.Ey, 46.65.+g

## I. INTRODUCTION

Transport processes and active motion in nature often consist of more than one motility state. Examples in biological systems include swimming of bacterial [1], migration of dendritic cells [2], chemical signal transport in neuronal dendrites [3], searching for specific target sites by DNA-binding proteins [4, 5], growth of biopolymers [6, 7], and motion of molecular motors along cytoskeleton [8]. While two-state transport processes are ubiquitous in nature, stochastic processes with multiple states have also been observed in natural systems, such as the three-state motion of *E. coli* near surfaces [9].

The dynamics of active particles is often described by the interplay between propulsion and stochastic forces in Langevin dynamics approaches. Alternatively, regardless of the origin of the exerted forces, a Langevin-type dynamics can be derived by replacing the forces with their impact on the particle kinematics reflected, e.g., in the reorientation statistics of the particle (the reorientations can be even controlled by an internal particle dynamics instead of external forces [10, 11]). This is a useful approach to extract the transport quantities of interest from the actual trajectory when the particle is tracked in a complex environment where various unknown forces may be exerted. However, the solvability of such models depends on the mathematical form of the turning-angle distribution, which usually restricts the analysis to specific regimes of motion such as the asymptotic long-term dynamics. Nevertheless, the intermediate- and short-time regimes of motion are often of particular interest and the time window of (biological) experiments is typically not wide enough to realize the long-term regime. Moreover, the reorientation statistics may have a complex form in

general. Thus, a general formalism to derive the time evolution of the transport quantities over all timescales for arbitrary turning-angle distributions is required which is technically challenging.

To model active dynamics with multiple states, simple combinations of stochastic processes—such as a ballistic flight and a pure diffusion—have been widely employed to capture some of the specific features of these systems [12–19]. A pertinent example is the bacterial dynamics, often modeled as ballistic run phases interrupted by periods of diffusion or random reorientation events, the so-called *run-and-tumble* dynamics [20–23]. The run trajectories are however curved (even spiral trajectories may form near surfaces [9]) and the run-phase persistence, duration, and speed vary with structural properties of bacteria or in response to environmental changes [1, 24, 25]. Also, tumbling is not a pure diffusion but rather an active phase with a reduced persistence; the flagellar bundles are only partially disrupted and there remains a weak swimming power to proceed forward [25, 26]. Therefore, a simplified ballistic-diffusive model for the bacterial dynamics is inadequate. A full description of such multistate stochastic processes requires a more complete formalism to combine multiple states of motion with arbitrary persistencies and speeds with the possibility of spontaneous transitions between the states.

Here we develop a general theoretical framework to combine distinct stochastic processes with arbitrary persistencies and speed distributions. We derive exact analytical expressions for the time evolution of arbitrary moments of displacement such as the mean square displacement (MSD) over all timescales. This enables us to link macroscopically observable transport properties, such as the long-term diffusion coefficient, to particle dynamics properties. By having access to the analytical form of the transport quantities we can optimize them with respect to the influential parameters, i.e. persistencies, speeds, and switching probabilities between the states.

---

\* shaebani@lusi.uni-sb.de

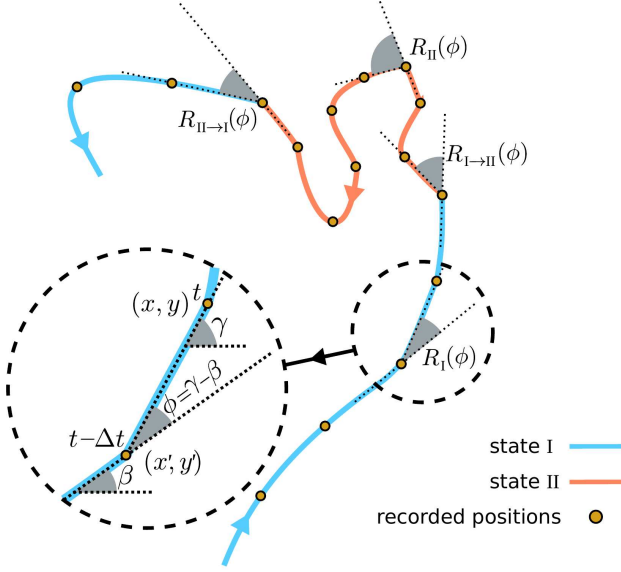


FIG. 1. A sample trajectory with two states of motion. The selected directional changes represent the four possible turning angles introduced in the model.

## II. MODEL

We consider a stochastic active process with two different modes of motility, characterized by their persistencies  $a_I$  and  $a_{II}$  and speed distributions  $F_I(v)$  and  $F_{II}(v)$ . While a two-state stochastic process is chosen as the most frequent multi-state process in natural systems, the formalism can be extended to processes with multiple states in general. We also note that a 2D active motion is studied here for brevity but nonetheless extension to 3D is straightforward (see e.g. [27] for 3D treatment of a single-state active process). By adopting a discrete-time process, our theoretical formalism and the results are directly applicable to the analysis of experimental data which often comprise a regularly-recorded discrete set of particle positions. Thus, the particle position along the trajectory is supposed to be recorded after successive time intervals of size  $\Delta t$ . We introduce four turning-angle distributions for the directional change  $\phi$  of the particle between successive time intervals of random walk [28, 29]:  $R_I(\phi)$  and  $R_{II}(\phi)$  for turning events within the states and  $R_{I \rightarrow II}(\phi)$  and  $R_{II \rightarrow I}(\phi)$  for changing the direction of motion when switching between the states (see Fig. 1). We quantify the persistence of the states by  $a_i = \int_{-\pi}^{\pi} d\phi e^{i\phi} R_i(\phi)$

and  $a_{II} = \int_{-\pi}^{\pi} d\phi e^{i\phi} R_{II}(\phi)$ . In many applications, turning-angle distributions are symmetric with respect to the arrival direction. In such cases, the persistencies reduce to real numbers  $a_i = \langle \cos \phi \rangle_{R_i}$  and  $a_{II} = \langle \cos \phi \rangle_{R_{II}}$ , thus, range within  $[-1, 1]$ . According to this generalized definition of the persistence, one obtains a positive  $a_i$  if  $R_i(\phi)$  is peaked around forward directions (persistent random walk). An isotropic  $R_i(\phi)$  leads to  $a_i = 0$  (normal diffusion) and a distribution which is peaked around backward directions leads to a negative  $a_i$  (anti-persistent random walk). The extreme values  $a_i = +1$  and  $-1$  correspond to a ballistic motion and a pure localization, respectively. For the general case of an asymmetric  $R_i(\phi)$ ,  $a_i$  has a nonzero imaginary part as well ( $a_i = \langle \cos \phi \rangle \pm i \langle \sin \phi \rangle$ ) which leads to a spiral trajectory [27] (as observed, e.g., for the dynamics of *E. coli* near surfaces [9]).

The particle switches stochastically between the two states with asymmetric probabilities  $f_{I \rightarrow II}$  and  $f_{II \rightarrow I}$ . Assuming constant transition probabilities  $f_{I \rightarrow II}$  and  $f_{II \rightarrow I}$  leads to exponential residence time distributions  $F_I(\tau) \sim e^{\ln(1-f_{I \rightarrow II})\tau}$  and  $F_{II}(\tau) \sim e^{\ln(1-f_{II \rightarrow I})\tau}$  with the mean residence times  $\langle \tau_I \rangle = 1/f_{I \rightarrow II}$  and  $\langle \tau_{II} \rangle = 1/f_{II \rightarrow I}$ . We assume that each switching event is accompanied by a change in the direction of motion according to the turning-angle distribution  $R_{I \rightarrow II}(\phi)$  or  $R_{II \rightarrow I}(\phi)$ . Similar to the persistencies, these directional changes at state-switching events can be quantified by the Fourier transforms  $\mathcal{R}_{I \rightarrow II} = \int_{-\pi}^{\pi} d\phi e^{i\phi} R_{I \rightarrow II}(\phi) = \langle \cos \phi \rangle_{R_{I \rightarrow II}}$  and  $\mathcal{R}_{II \rightarrow I} = \int_{-\pi}^{\pi} d\phi e^{i\phi} R_{II \rightarrow I}(\phi) = \langle \cos \phi \rangle_{R_{II \rightarrow I}}$ . A turning measure  $\mathcal{R}_{i \rightarrow j}$  close to 1, -1, or 0 corresponds, respectively, to slightly changing, reversing, or randomizing the direction of motion when switching from state  $i$  to  $j$ .

## III. EVOLUTION OF THE MOMENTS OF DISPLACEMENT

We introduce  $P_t^I(x, y|\gamma)$  and  $P_t^{II}(x, y|\gamma)$  as the conditional probability density functions to find the particle at position  $(x, y)$  along the direction  $\gamma$  at time  $t$  in each state of motion. The total probability density  $P_t(x, y|\gamma)$  is then given by  $P_t(x, y|\gamma) = P_t^I(x, y|\gamma) + P_t^{II}(x, y|\gamma)$ . The state of the system at successive time intervals  $t - \Delta t$  and  $t$  is given by  $\begin{bmatrix} P_{t-\Delta t}^I(x', y'|\beta) \\ P_{t-\Delta t}^{II}(x', y'|\beta) \end{bmatrix}$  and  $\begin{bmatrix} P_t^I(x, y|\gamma) \\ P_t^{II}(x, y|\gamma) \end{bmatrix}$ , with  $x' = x - v\Delta t \cos \gamma$ ,  $y' = y - v\Delta t \sin \gamma$ ; see Fig. 1. The temporal evolution of the stochastic process can be described by the following set of master equations for the probability densities:

$$\begin{bmatrix} P_t^I(x, y|\gamma) \\ P_t^{II}(x, y|\gamma) \end{bmatrix} = \int dv \int_{-\pi}^{\pi} d\beta \begin{bmatrix} (1-f_{I \rightarrow II})F_I(v)R_I(\gamma-\beta) & f_{II \rightarrow I}F_{II}(v)R_{II \rightarrow I}(\gamma-\beta) \\ f_{I \rightarrow II}F_I(v)R_{I \rightarrow II}(\gamma-\beta) & (1-f_{II \rightarrow I})F_{II}(v)R_{II}(\gamma-\beta) \end{bmatrix} \begin{bmatrix} P_{t-\Delta t}^I(x', y'|\beta) \\ P_{t-\Delta t}^{II}(x', y'|\beta) \end{bmatrix}. \quad (1)$$

Each of the master equations consists of two terms on the right hand side, which represent the possibility of being in each of the two states in the previous time step. The change in the direction of motion, i.e.  $\phi = \gamma - \beta$ , is randomly chosen from the four turning-angle distributions. Here, the speed and turning-angle distributions are supposed to be independent for simplicity; however, persistence and speed can be correlated in general [30]. Using the Fourier transform of the probability density function  $P_t(\mathbf{k}|m) = \int_{-\pi}^{\pi} d\gamma e^{im\gamma} \int dy \int dx e^{i\mathbf{k} \cdot \mathbf{r}} (P_t^I(x, y|\gamma) + P_t^{\text{II}}(x, y|\gamma))$ , the moments of displacement can be extracted as

$$\langle x^a y^b \rangle(t) = (-i)^{a+b} \frac{\partial^{a+b} P_t(k_x, k_y|m=0)}{\partial k_x^a \partial k_y^b} \Big|_{(k_x, k_y)=(0,0)}. \quad (2)$$

For example, using the polar representation of  $\mathbf{k}$  as  $(k, \theta)$ , the MSD can be calculated as  $\langle r^2 \rangle(t) = (-i)^2 \frac{\partial^2 P_t(k, \theta=0|m=0)}{\partial k^2} \Big|_{k=0}$ . The Fourier transform of the master equations (1) leads to

$$P_t^I(k, \theta|m) = \int dv F_1(v) \times \left[ (1 - f_{I \rightarrow \text{II}}) \int d\gamma e^{im\gamma} \int d\beta R_1(\gamma - \beta) \int dy \int dx e^{i\mathbf{k} \cdot \mathbf{r}} P_{t-\Delta t}^I(x', y'|\beta) + f_{\text{II} \rightarrow I} \int d\gamma e^{im\gamma} \int d\beta R_{\text{II} \rightarrow I}(\gamma - \beta) \int dy \int dx e^{i\mathbf{k} \cdot \mathbf{r}} P_{t-\Delta t}^{\text{II}}(x', y'|\beta) \right], \quad (3)$$

and a similar equation for  $P_t^{\text{II}}(k, \theta|m)$ . Next, using the  $q$ -th order Bessel's function  $J_q(z) = \frac{1}{2\pi i^q} \int_{-\pi}^{\pi} d\gamma e^{iz \cos \gamma} e^{-iq\gamma}$ , the probability densities in the Fourier space can be expanded as a Taylor series in powers of  $k$  [31]. By collecting all terms with the same power in  $k$ , we obtain a set of coupled equations for the  $q$ -th expansion coefficient  $Q_{q,t}^I(\theta|m)$  or  $Q_{q,t}^{\text{II}}(\theta|m)$ . For example, for the terms with power 0 in  $k$  we obtain

$$\begin{aligned} Q_{0,t}^I(\theta|m) &= (1 - f_{I \rightarrow \text{II}}) R_1(m) Q_{0,t-\Delta t}^I(\theta|m) \\ &\quad + f_{\text{II} \rightarrow I} R_{\text{II} \rightarrow I}(m) Q_{0,t-\Delta t}^{\text{II}}(\theta|m), \\ Q_{0,t}^{\text{II}}(\theta|m) &= (1 - f_{\text{II} \rightarrow I}) R_{\text{II}}(m) Q_{0,t-\Delta t}^{\text{II}}(\theta|m) \\ &\quad + f_{I \rightarrow \text{II}} R_{I \rightarrow \text{II}}(m) Q_{0,t-\Delta t}^I(\theta|m). \end{aligned} \quad (4)$$

The expansion coefficients of terms with higher powers in  $k$  can be similarly calculated. The resulting set of coupled equations for each expansion coefficient connect time steps  $t$  and  $t - \Delta t$  and can be solved by applying a  $z$ -transform  $Q(z) = \sum_{t=0}^{\infty} Q_t z^{-t}$ . This powerful analytical technique enables us to derive an exact expression for any arbitrary moment of displacement  $\langle x^q \rangle(z)$  from the corresponding expansion coefficients as  $\langle x^q \rangle(z) = \sum_{j \in \{I, \text{II}\}} \langle v_j^q \rangle (\Delta t)^q Q_q^j(z, 0|0)$ . For instance, the

MSD has the following relation with the coefficients of terms with power 2 in  $k$ , i.e.  $Q_2^I(z, \theta|m)$  and  $Q_2^{\text{II}}(z, \theta|m)$ :

$$\langle r^2 \rangle(z) = 2(\Delta t)^2 \left( \langle v_I^2 \rangle Q_2^I(z, 0|0) + \langle v_{\text{II}}^2 \rangle Q_2^{\text{II}}(z, 0|0) \right). \quad (5)$$

Using a Fourier- $z$ -transform technique [27, 31], after some calculations we obtain the following exact expression for the MSD in the  $z$ -space

$$\begin{aligned} \langle x^2 \rangle(z) &= \frac{(\Delta t)^2}{z-1} \sum_{j \in \{I, \text{II}\}, j \neq j'} \frac{z^2 f_{j' \rightarrow j} + (z^2 - z)(1 - f_{j \rightarrow j'} - f_{j' \rightarrow j}) P_0^j}{G_0(z)} \times \\ &\quad \left[ \frac{z [z - (1 - f_{j' \rightarrow j}) a_{j'}] \langle v_j \rangle^2}{G_1(z)} + \frac{z f_{j \rightarrow j'} \mathcal{R}_{j \rightarrow j'} \langle v_j \rangle \langle v_{j'} \rangle}{G_1(z)} - \langle v_j \rangle^2 + \frac{\langle v_j^2 \rangle}{2} \right], \end{aligned} \quad (6)$$

where  $G_1(z) = \prod_{j \in \{I, \text{II}\}} [z - (1 - f_{j \rightarrow j'}) a_j] - \prod_{j \in \{I, \text{II}\}} f_{j \rightarrow j'} \mathcal{R}_{j \rightarrow j'}$ ,  $G_0(z) = (z-1)(z-1 + f_{\text{II} \rightarrow I} + f_{I \rightarrow \text{II}})$ , and  $P_0^j$  is the probability of initially starting in state  $j$  ( $P_0^I + P_0^{\text{II}} = 1$ ). Note that  $\Delta t$  can be absorbed into the speed terms in the above equation to construct the mean step length  $\langle \ell_j \rangle = \langle v_j \Delta t \rangle$  or the second moment of step length  $\langle \ell_j^2 \rangle = \langle v_j^2 (\Delta t)^2 \rangle$  in state  $j$ . By the inverse  $z$ -transform of Eq. (6), one can straightforwardly obtain an exact expression for the MSD in real time, i.e.  $\langle x^2 \rangle(t)$ . However, in contrast to the compact form of the MSD in  $z$  space,  $\langle x^2 \rangle(t)$  is too lengthy to present here. The general expression of  $\langle x^2 \rangle(t)$  consists of an exponentially-decaying term with  $t$ , a time-independent term, and a term which grows linearly with  $t$ . While the short-time dynamics is mainly controlled by the exponentially-decaying and time-independent terms, the contribution of the linear term dominates at long times. It turns out that the initial condition  $P_0^j$  only influences the time-independent and exponentially-decaying terms of the MSD, thus, diversifies the anomalous dynamics on short time scales.

The Markov process of transitions between the two states exponentially approaches the steady probabilities  $P_s^I = \frac{f_{\text{II} \rightarrow I}}{f_{I \rightarrow \text{II}} + f_{\text{II} \rightarrow I}}$  and  $P_s^{\text{II}} = \frac{f_{I \rightarrow \text{II}}}{f_{I \rightarrow \text{II}} + f_{\text{II} \rightarrow I}}$  with the characteristic time

$$t_s = \frac{-1}{\ln |1 - f_{I \rightarrow \text{II}} - f_{\text{II} \rightarrow I}|}. \quad (7)$$

In the following we choose  $P_0^j = P_s^j$ , i.e. an initially equilibrated system. While this choice reduced the complexity of the short-time dynamics by excluding the role of the initial conditions of motion, Fig. 2(a) shows that a wide range of different types of anomalous dynamics is still observed on varying other key parameters. The shape of MSD profiles strongly depends on the choice of persistence parameters and switching probabilities. Also the speed heterogeneities nontrivially push the initial slope toward the ordinary diffusion line by increasing the role of the linear terms of the MSD. When the motion in one or both states is strongly antipersistent, an oscillatory dynamics at short timescales emerges [32, 33]. In some parameter regimes, the exponential terms of the MSD rapidly decay and time-independent terms develop a plateau regime over intermediate timescales. Also note that the profiles for different initial conditions  $P_0^j$  merge at long times, when the crossover to asymptotic diffusive

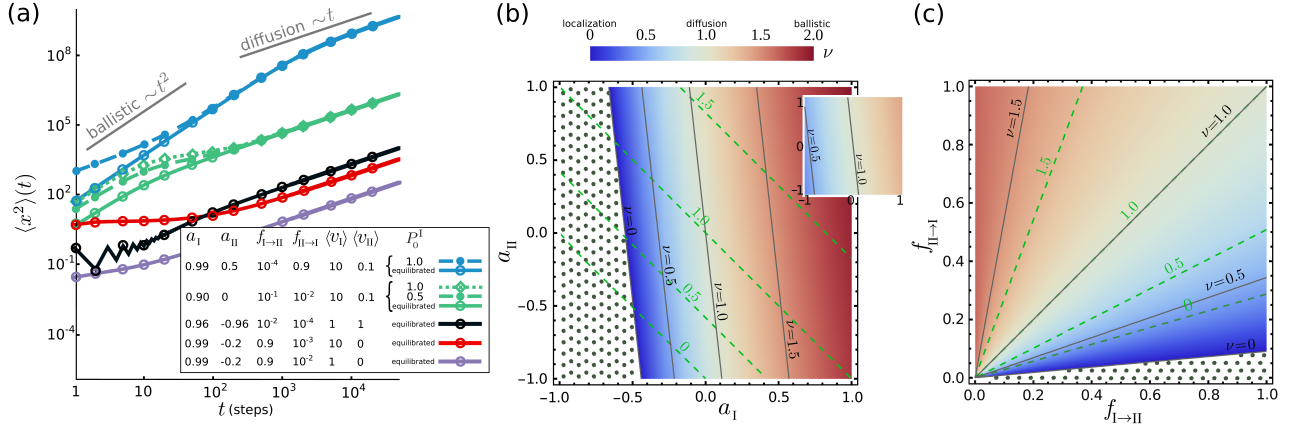


FIG. 2. (a) Time evolution of the MSD. The speed of each state is constant, except for the upper dash-dotted curve with speed heterogeneity  $\langle v^2 \rangle / \langle v \rangle^2 = 20$  in both states. The symbols denote simulation results and the lines correspond to analytical predictions via Eq. (6). The solid, dashed, and dotted curves represent different initial probability  $P_0^I$  of starting the motion in state I. (b),(c) Phase diagrams of the initial anomalous exponent in  $(a_I, a_{II})$  and  $(f_{I-II}, f_{II-I})$  planes. The color intensity reflects the magnitude of  $\nu$ , with red (blue) meaning superdiffusion (subdiffusion). The dotted regions denote oscillatory subdomains. A constant speed is considered except for the inset with the speed heterogeneity  $\langle v_j^2 \rangle / \langle v_j \rangle^2 = 3$ . The parameter values in panel (b) are  $f_{I-II} = 0.1$  and  $f_{II-I} = 0.9$  and the green contour lines correspond to parameter values  $f_{I-II} = f_{II-I} = 0.5$ . In panel (c), the parameter values are  $a_I = 0.6$ ,  $a_{II} = -0.6$  (green contour lines:  $a_I = 0.9$ ,  $a_{II} = -0.9$ ).

dynamics occurs. To confirm the validity of the analytical predictions we perform extensive Monte Carlo simulations of the same stochastic process. We consider a 2D random walk with two different modes of motion and allow the walker to spontaneously change the mode of motion at each timestep according to given asymmetric transition probabilities. Figure 2(a) shows the simulation results, averaged over an ensemble of  $10^5$  realizations. The simulation results agree perfectly with the analytical predictions.

#### IV. INITIAL ANOMALOUS EXPONENT

The transient dynamics is of particular interest as the time window of experiments is practically limited. The initial part of the MSD can be fitted to a power-law  $\langle r^2 \rangle(t) \sim t^\nu$  to derive the initial anomalous exponent

$$\nu = 1 + \ln \left[ 1 + \frac{\sum_j \langle v_j \rangle f_{j \rightarrow j} [f_{j \rightarrow j} \mathcal{R}_{j \rightarrow j} \langle v_j \rangle + (1 - f_{j \rightarrow j}) a_j \langle v_j \rangle]}{\sum_{j \in \{I, II\}} f_{j \rightarrow j} \langle v_j \rangle^2} \right] / \ln 2. \quad (8)$$

For a single-state active motion, it reduces to  $\nu = 1 + \frac{\ln(1+a)}{\ln 2}$  [28]. The phase diagrams in Fig. 2(b),(c) represent the variations of  $\nu$  in the parameters space. The onset of oscillatory dynamics can be identified by setting  $\nu = 0$ .

#### V. CROSSOVER TIME TO THE LONG-TERM DIFFUSION

The long-term dynamics is diffusion since the walker gradually loses its memory of the initial direction and state of motion, and the trajectory eventually gets randomized. The probability density of a persistent random walk was shown to follow an asymptotic Gaussian form [34]. We find that the MSD exponentially converges to the asymptotic diffusive regime as

$$\langle r^2 \rangle(t) - \langle r^2 \rangle(t \rightarrow \infty) \sim b_1 e^{-t/t_s} + b_2 e^{-t/t_{c+}} + b_3 e^{-t/t_{c-}}, \quad (9)$$

with characteristic times  $t_s$  [Eq. (7)] and

$$t_{c\pm} = \frac{-1}{\ln \left| \frac{2 - \lambda_I - \lambda_{II} \pm \sqrt{(\lambda_{II} - \lambda_I)^2 + \mathcal{C}}}{2} \right|}, \quad (10)$$

where  $\lambda_j = 1 - a_j(1 - f_{j \rightarrow j'})$  and  $\mathcal{C} = \prod_{j \in \{I, II\}} 2f_{j \rightarrow j'} \mathcal{R}_{j \rightarrow j'}$ . Thus, the crossover time is determined in general by the probabilities  $f_{j \rightarrow j'}$ , turning measures  $\mathcal{R}_{j \rightarrow j'}$  at switchings, and the persistence parameters  $a_j$ , as shown in Fig. 3. The crossover time to the asymptotic regime is controlled by the longest characteristic time and can vary by several orders of magnitude within the relevant control parameter ranges. Other parameters may also be influential, since the prefactors  $b_1$ ,  $b_2$ , and  $b_3$  depend on all parameters including the first two moments of the speeds  $v_i$  and  $v_{II}$  as well as the initial conditions  $P_0^j$ .



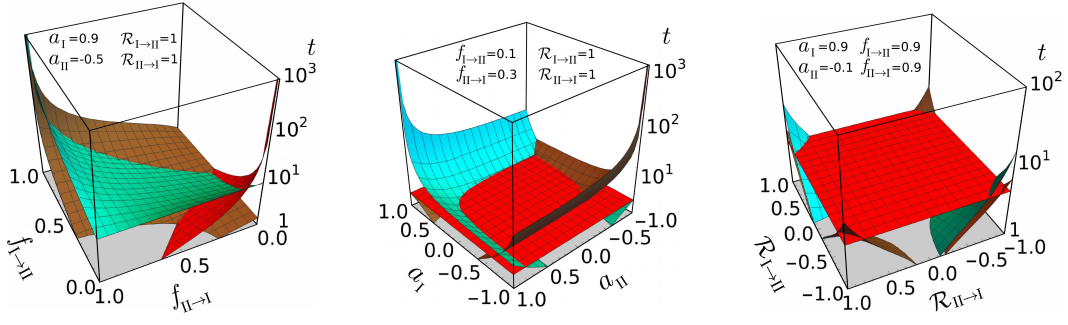


FIG. 3. Characteristic times  $t_s$ ,  $t_{c+}$ , and  $t_{c-}$  (red, cyan, and brown surfaces, respectively) in different parameters space.

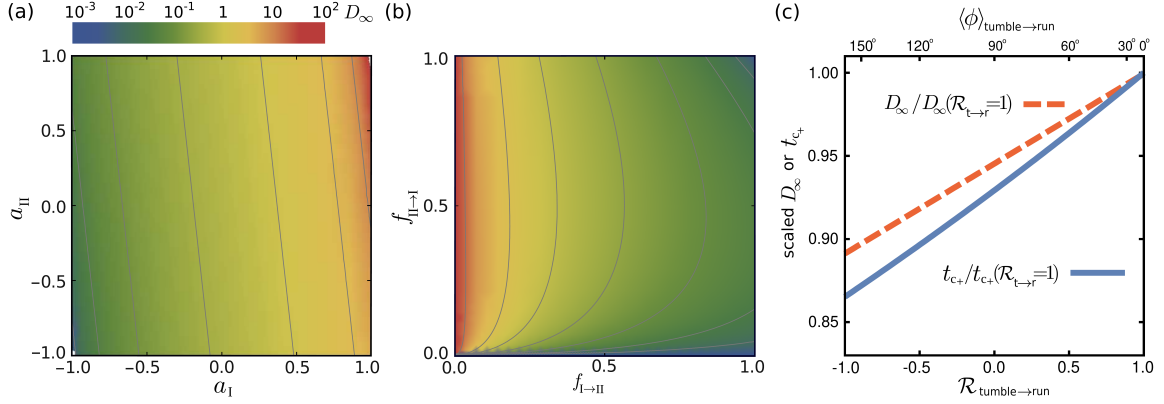


FIG. 4. (a),(b)  $D_\infty$  in  $(a_I, a_{II})$  and  $(f_{I \to II}, f_{II \to I})$  planes, for a constant speed and the parameter values (unless varied):  $f_{I \to II}=0.1$ ,  $f_{II \to I}=0.9$ ,  $a_I=0.9$ ,  $a_{II}=-0.9$ ,  $R_{II \to I}=a_I$ ,  $R_{I \to II}=a_{II}$ . (c) Variations of  $D_\infty$  and  $t_{c+}$  in a run-and-tumble process in terms of the mean *tumble-to-run* turning angle  $\langle \phi \rangle_{\text{tumble} \rightarrow \text{run}}$  (correspondingly  $\mathcal{R}_{\text{tumble} \rightarrow \text{run}}$ ). Other parameter values:  $f_{r \rightarrow t}=f_{t \rightarrow r}=0.1$ ,  $a_r=0.9$ ,  $a_t=0$ ,  $\mathcal{R}_{r \rightarrow t}=1$ , and  $v_r=2v_t$ .

## VI. ASYMPTOTIC DIFFUSION CONSTANT

The MSD in the long-time limit  $\langle r^2 \rangle(t \rightarrow \infty)$  grows linearly with  $t$ , with a prefactor from which the long-term diffusion coefficient can be deduced as

$$D_\infty = \frac{\Delta t}{\sum_{j \in \{I, II\}} 4 f_{j \rightarrow j'} (\lambda_j \lambda_{j'} - C)} \sum_{j \in \{I, II\}} f_{j \rightarrow j'} \left[ 2 f_{j' \rightarrow j} \mathcal{R}_{j \rightarrow j'} \langle v_j \rangle \langle v_{j'} \rangle - C \Delta v_{j'} + \lambda_j \lambda_{j'} \langle v_{j'}^2 \rangle + 2 a_{j'} \lambda_j (1 - f_{j' \rightarrow j}) \langle v_{j'} \rangle^2 \right], \quad (11)$$

where  $\Delta v_j = \langle v_j^2 \rangle - 2 \langle v_j \rangle^2$ . To clarify how  $D_\infty$  depends on the key parameters  $a_j$  and  $f_{j \rightarrow j'}$ , we consider a process in which the walker smoothly enters the new state, i.e. without experiencing a directional change; thus,  $\mathcal{R}_{II \rightarrow I} = a_I$  and  $\mathcal{R}_{I \rightarrow II} = a_{II}$ . As shown in Figs. 4(a),(b),  $D_\infty$  varies by several orders of magnitude by changing the key parameters. Equation (11) describes  $D_\infty$  for any arbitrary combination of the stochastic processes. For instance, for a simple combination of pure diffusion (with constant  $D_1$ ) and waiting, Eq. (11) reduces to  $D_\infty = D_1 \frac{f_{II \rightarrow I}}{f_{I \rightarrow II} + f_{II \rightarrow I}}$ , which was originally shown by Lennard-Jones for surface diffusion with traps [35].  $D_\infty$  is independent of the initial

conditions  $P_0^j$ , implying that the history of the process is only carried by exponential and time-independent terms of the MSD that are negligible at long times as the linear term eventually dominates.

## VII. APPLICATIONS AND SPECIAL CASES

The broad applicability of our formalism enables us to make generic predictions about the dynamics of various systems. In this section we present a few applications and the reduced form of the general analytical expressions for a couple of specific choices for the states of motion.

*Bacterial dynamics*— Bacterial species that swim by the rotation of flagella experience an alternating sequence of run and tumble phases. An abrupt directional change often occurs when switching back from tumble to run phase [1, 25], which is caused by the torque exerted on the cell body during the reformation of the bundle [36]. It is hypothesized that the bacteria benefit from this feature to slow their spreading and explore the environment more efficiently. Since in our model the statistics of the turning angles at the switching events are chosen to be independent from the turning angles within the states in

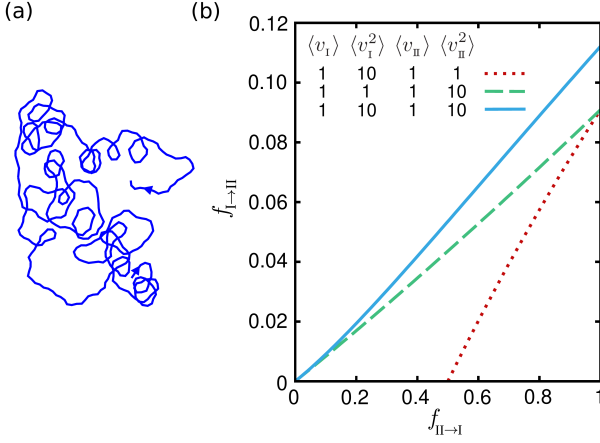


FIG. 5. (a) Typical trajectory of a single-state persistent walker with the asymmetric turning-angle distribution given in the text. The resulting persistence parameter has real and imaginary parts  $a_R \simeq 0.9$  and  $a_I \simeq 0.2$ , respectively. (b) Subset of optimal switching probabilities  $f_{I \rightarrow II}^{opt}$  and  $f_{II \rightarrow I}^{opt}$  in the  $(f_{I \rightarrow II}, f_{II \rightarrow I})$  plane for various choices of speed dispersions in a combination of ballistic and diffusive processes.

general, we can directly check how directional changes at the switching events influence the crossover time to the long-term diffusive dynamics and the asymptotic diffusion coefficient. Figure 4(c) shows that increasing the mean directional change at switching from tumble to run,  $\langle \phi \rangle_{\text{tumble} \rightarrow \text{run}}$ , helps the bacteria to randomize their path: A stronger kick (i.e. a larger turning angle  $\langle \phi \rangle_{\text{tumble} \rightarrow \text{run}}$ ) can decrease the characteristic time  $t_{c+}$  and the diffusion coefficient  $D_\infty$  even by more than 20%, which is expected to substantially affect the first-passage properties and the ability to efficiently explore the environment.

*Spiral trajectories*— The distribution  $R(\phi)$  of the turning angles  $\phi$  with respect to the arrival direction can be asymmetric in general. In such a case, the imaginary part of the persistence, i.e.  $\int_{-\pi}^{\pi} d\phi \sin(\phi) R(\phi)$ , is nonzero and the persistence can be written as  $a = \langle \cos \phi \rangle \pm i \langle \sin \phi \rangle$ .

If we consider a single-state 2D motion for simplicity, an asymmetric  $R(\phi)$  means that the left-right symmetry does not hold and the particle turns more frequently either to the right or to the left direction, leading to the emergence of clockwise or anti-clockwise spiral trajectories. For example, motion with a uniform distribution  $R(\phi) = \frac{1}{\pi/2}$  but over an asymmetric range  $[-\frac{\pi}{6}, \frac{2\pi}{6}]$  of  $\phi$  corresponds to a trajectory with frequent clockwise spirals [see Fig. 5(a)]. Denoting the real and imaginary parts of the persistence  $a$ , respectively, with  $a_R$  and  $a_I$ , the asymptotic diffusion coefficient for a single-state process can be deduced as

$$D_\infty = \frac{1}{4} v^2 \Delta t \frac{(1-a_R^2)-a_I^2}{(1-a_R)^2+a_I^2}, \quad (12)$$

where we choose a constant speed  $v$  for simplicity. It can be seen that the asymmetric contribution reduces the asymptotic diffusion coefficient. If we denote the diffusion coefficient of a normal diffusion with  $D_0 = \frac{1}{4} v^2 \Delta t$ ,  $D_\infty$  is larger than  $D_0$  if  $a_I < \sqrt{a_R(1-a_R)}$ ; otherwise, the spread is slower than the normal diffusion even though the propulsion  $a_R$  is present. A constraint for a pure localization ( $D_\infty = 0$ ) can be obtained as  $a_R^2 + a_I^2 = 1$ .

*Run-and-tumble dynamics*— A subclass of two-state processes of particular interest is a combination of fast and slow dynamics, described by the so-called *run-and-tumble* models [20–23]. The modeling of such processes has been often limited either to extract the long-term dynamics of the particle or to simplify the states with stochastic processes such as ballistic motion and normal diffusion. However, as we described in the previous sections, our formalism enables us to combine two states with arbitrary persistencies and describe the particle dynamics over all time scales. The general form of the expressions presented in the previous sections can be reduced to shorter formulas for specific choices of the two processes. Here we choose a normal diffusion  $a_{II} = 0$  for the dynamics of the slow state as an example. Then, the general explicit form of the time evolution of MSD reduces to

$$\begin{aligned} \langle r^2 \rangle(t) = & \frac{a_I^2 (f_{I \rightarrow II} - 1) \left( (f_{II \rightarrow I} + f_{I \rightarrow II}) (f_{II \rightarrow I} - 1) + (f_{I \rightarrow II} - 3) f_{I \rightarrow II} \right) + 2 f_{I \rightarrow II}}{(a_I (f_{I \rightarrow II} - 1) (f_{II \rightarrow I} + f_{I \rightarrow II}) + f_{II \rightarrow I} + f_{I \rightarrow II})^2} \\ & + \frac{\left( a_I ((f_{II \rightarrow I} - 1) f_{I \rightarrow II} + f_{II \rightarrow I} + f_{I \rightarrow II}^2) + f_{II \rightarrow I} + f_{I \rightarrow II} \right)}{a_I (f_{I \rightarrow II} - 1) (f_{II \rightarrow I} + f_{I \rightarrow II}) + f_{II \rightarrow I} + f_{I \rightarrow II}} t - \frac{2 a_I (f_{I \rightarrow II} - 1) (f_{I \rightarrow II} a_I (f_{II \rightarrow I} + f_{I \rightarrow II} - 2) + f_{II \rightarrow I} + f_{I \rightarrow II} + a_I - 1) (a_I (1 - f_{I \rightarrow II}))^t}{(a_I (f_{I \rightarrow II} - 1) + 1)^2 (f_{II \rightarrow I} - f_{I \rightarrow II} a_I + f_{I \rightarrow II} + a_I - 1)} + \\ & \frac{2 a_I f_{I \rightarrow II} (1 - f_{II \rightarrow I} - f_{I \rightarrow II})^{t+2}}{(f_{II \rightarrow I} + f_{I \rightarrow II})^2 (f_{II \rightarrow I} - f_{I \rightarrow II} a_I + f_{I \rightarrow II} + a_I - 1)} + \frac{\left( a_I ((f_{II \rightarrow I} - 1) f_{I \rightarrow II} + f_{II \rightarrow I} + f_{I \rightarrow II}^2) + f_{II \rightarrow I} + f_{I \rightarrow II} \right)}{a_I (f_{I \rightarrow II} - 1) (f_{II \rightarrow I} + f_{I \rightarrow II}) + f_{II \rightarrow I} + f_{I \rightarrow II}} - \frac{2 a_I ((f_{II \rightarrow I} + f_{I \rightarrow II})^2 - f_{I \rightarrow II}) + (f_{II \rightarrow I} + f_{I \rightarrow II})^2}{(a_I (f_{I \rightarrow II} - 1) (f_{II \rightarrow I} + f_{I \rightarrow II}) + f_{II \rightarrow I} + f_{I \rightarrow II})^2}. \end{aligned} \quad (13)$$

While the other transport quantities of interest can be also presented in a shorter form by this specific choice,

the advantage of our formalism is that other features of

the motion can be still kept in their general form. Particularly, the fast state is a persistent motion described by  $a_I$  (and not a simple ballistic motion necessarily) and the speeds of both states are described by their distributions (and not assumed to be constant). For example, we obtain from Eq. (11) the following reduced form for the asymptotic diffusion coefficient in case of smooth transitions between the states (i.e. when  $\mathcal{R}_{I \rightarrow \Pi} = a_{\Pi} = 0$  and  $\mathcal{R}_{\Pi \rightarrow I} = a_I$ ):

$$D_{\infty} = \frac{\Delta t}{4} \left[ \frac{f_{I \rightarrow \Pi}}{f_{I \rightarrow \Pi} + f_{\Pi \rightarrow I}} \langle v_{\Pi}^2 \rangle + \frac{(f_{I \rightarrow \Pi} - 1)f_{\Pi \rightarrow I} a_I \Delta v_I + f_{\Pi \rightarrow I} \langle v_I^2 \rangle + 2 f_{I \rightarrow \Pi} f_{\Pi \rightarrow I} a_I \langle v_I \rangle \langle v_{\Pi} \rangle}{(f_{I \rightarrow \Pi} + f_{\Pi \rightarrow I}) (1 - a_I (1 - f_{I \rightarrow \Pi}))} \right], \quad (14)$$

with  $\Delta v_I = \langle v_I^2 \rangle - 2 \langle v_I \rangle^2$ . For the explicit form of  $D_{\infty}$  in a ballistic-diffusive process, one readily replaces  $a_I = 1$  in the above equation. Note that Eq. (14) also describes a combination of diffusion and subdiffusion for  $-1 < a_I < 0$ .

*Optimization of transport quantities*—The advantage of having the explicit analytical form of the transport quantities of interest is that analytical expressions can be also extracted for the derivatives with respect to any control parameter, which makes the optimization of the transport quantities feasible. For example, the asymptotic diffusion coefficient given in Eq. (14) can be minimized with respect to the switching probabilities using e.g.

$$\left. \frac{\partial D_{\infty}}{\partial f_{I \rightarrow \Pi}} \right|_{f_{I \rightarrow \Pi} = f_{I \rightarrow \Pi}^{\text{opt}}} = 0, \quad (15)$$

to obtain the following relation between the optimal switching probabilities  $f_{I \rightarrow \Pi}^{\text{opt}}$  and  $f_{\Pi \rightarrow I}^{\text{opt}}$  in a combination

of ballistic ( $a_I = 1$ ) and diffusive ( $a_{\Pi} = 0$ ) processes

$$f_{I \rightarrow \Pi}^{\text{opt}} = \frac{-2 f_{\Pi \rightarrow I}^{\text{opt}} \langle v_I \rangle^2 + f_{\Pi \rightarrow I}^{\text{opt}} \sqrt{B - 2 \langle v_I \rangle^2}}{B}, \quad (16)$$

with  $B = f_{\Pi \rightarrow I}^{\text{opt}} \Delta v_I + 2 f_{\Pi \rightarrow I}^{\text{opt}} \langle v_I \rangle \langle v_{\Pi} \rangle + \langle v_{\Pi}^2 \rangle$ . We find the necessary condition  $B \geq 4 \langle v_I \rangle^4 + 2 \langle v_I \rangle^2$  for having an optimal solution. Figure 5(b) shows a few optimal paths in the  $(f_{I \rightarrow \Pi}, f_{\Pi \rightarrow I})$  plane for various choices of speed dispersion in each state.

## VIII. CONCLUSION

We developed an analytical framework which provides a quantitative link between the characteristics of particle dynamics in a two-state active process and macroscopically observable transport properties. The method can be straightforwardly extended to three dimensions and multistate stochastic processes. We disentangled the combined effects of speed, directional persistence, and switching statistics on the transport quantities of interest. The extracted exact expressions for the time evolution of the moments of displacement make it possible to also express other transport quantities by a cumulant expansion in terms of the moments of displacement. The broad applicability of our approach makes it applicable to diverse transport problems in active matter systems as well as passive processes such as clogging dynamics in granular media and microbial populations, chromatography, and transport in amorphous materials.

## IX. ACKNOWLEDGMENTS

We acknowledge support from the Deutsche Forschungsgemeinschaft (DFG) through the collaborative research center SFB 1027. MRS acknowledges support by Saarland University NanoBioMed initiative Grant No. 7410110401.

- 
- [1] H. C. Berg, *E. coli in motion* (Springer Verlag, New York, 2004).
  - [2] M. Chabaud et al., Nat. Commun. **6**, 7526 (2015).
  - [3] R. Jose, L. Santen, and M. R. Shaebani, Biophys. J. **115**, 2014 (2018).
  - [4] M. Bauer and R. Metzler, Biophys. J. **102**, 2321 (2012).
  - [5] Y. Meroz, I. Eliazar, and J. Klafter, J. Phys. A **42**, 434012 (2009).
  - [6] M. Dogterom and S. Leibler, Phys. Rev. Lett. **70**, 1347 (1993).
  - [7] M. R. Shaebani, P. Aravind, O. Albrecht, and S. Ludger, Sci. Rep. **6**, 30285 (2016).
  - [8] S. Klumpp and R. Lipowsky, Phys. Rev. Lett. **95**, 268102 (2005).
  - [9] E. Perez Ipina, S. Otte, R. Pontier-Bres, D. Czerucka, and F. Peruani, Nat. Phys. **15**, 610 (2019).
  - [10] L. G. Nava, R. Großmann, and F. Peruani, Phys. Rev. E **97**, 042604 (2018).
  - [11] L. Gómez Nava, T. Goudon, and F. Peruani, Math. Models Methods Appl. Sci. **31**, 1691 (2021).
  - [12] P. C. Bressloff and J. M. Newby, Rev. Mod. Phys. **85**, 135 (2013).
  - [13] A. E. Hafner, L. Santen, H. Rieger, and M. R. Shaebani, Sci. Rep. **6**, 37162 (2016).
  - [14] J. Taktikos, H. Stark, and V. Zaburdaev, PLOS ONE **8**, 1 (2013).
  - [15] I. Pinkoviezky and N. S. Gov, Phys. Rev. E **88**, 022714 (2013).

- [16] M. R. Shaebani, R. Jose, C. Sand, and L. Santen, *Phys. Rev. E* **98**, 042315 (2018).
- [17] N. Watari and R. G. Larson, *Biophys. J.* **98**, 12 (2010).
- [18] M. Theves, J. Taktikos, V. Zaburdaev, H. Stark, and C. Beta, *Biophys. J.* **105**, 1915 (2013).
- [19] M. R. Shaebani and H. Rieger, *Front. Phys.* **7**, 120 (2019).
- [20] L. Angelani, R. Di Leonardo, and G. Ruocco, *Phys. Rev. Lett.* **102**, 048104 (2009).
- [21] J. Elgeti and G. Gompper, *EPL* **109**, 58003 (2015).
- [22] F. Thiel, L. Schimansky-Geier, and I. M. Sokolov, *Phys. Rev. E* **86**, 021117 (2012).
- [23] L. Angelani, *EPL* **102**, 20004 (2013).
- [24] A. E. Patteson, A. Gopinath, M. Goulian, and P. E. Arratia, *Sci. Rep.* **5**, 15761 (2015).
- [25] J. Najafi, M. R. Shaebani, T. John, F. Altegoer, G. Bange, and C. Wagner, *Science Adv.* **4**, eaar6425 (2018).
- [26] L. Turner, L. Ping, M. Neubauer, and H. C. Berg, *Biophys. J.* **111**, 630 (2016).
- [27] Z. Sadjadi, M. R. Shaebani, H. Rieger, and L. Santen, *Phys. Rev. E* **91**, 062715 (2015).
- [28] M. R. Shaebani, Z. Sadjadi, I. M. Sokolov, H. Rieger, and L. Santen, *Phys. Rev. E* **90**, 030701 (2014).
- [29] S. Burov, S. M. A. Tabei, T. Huynh, M. P. Murrell, L. H. Philipson, S. A. Rice, M. L. Gardel, N. F. Scherer, and A. R. Dinner, *Proc. Natl. Acad. Sci. USA* **110**, 19689 (2013).
- [30] M. R. Shaebani, R. Jose, L. Santen, L. Stankevics, and F. Lautenschläger, *Phys. Rev. Lett.* **125**, 268102 (2020).
- [31] Z. Sadjadi, M. Miri, M. R. Shaebani, and S. Nakhaee, *Phys. Rev. E* **78**, 031121 (2008).
- [32] P. Tierno, F. Sagués, T. H. Johansen, and I. M. Sokolov, *Phys. Rev. Lett.* **109**, 070601 (2012).
- [33] P. Tierno and M. R. Shaebani, *Soft Matter* **12**, 3398 (2016).
- [34] G. H. Weiss, *J. Stat. Phys.* **15**, 157 (1976).
- [35] J. E. Lennard-Jones, *Trans. Faraday Soc.* **28**, 333 (1932).
- [36] N. C. Darnton, L. Turner, S. Rojevsky, and H. C. Berg, *J. Bacteriol.* **189**, 1756 (2007).